0013-7227/99/$03.00/0
Endocrinology

Vol. 140, No. 6
Printed in U.S.A.

Targeted Disruption of the Estrogen Receptor-α Gene in Female Mice: Characterization of Ovarian Responses and Phenotype in the Adult*

DAVID W. SCHOMBERG, JOHN F. COUSE, ABIR MUKHERJEE, DENNIS B. LUBAHN, M. SAR, KELLY E. MAYO, AND KENNETH S. KORACH

Departments of Obstetrics and Gynecology and Cell Biology (D.W.S.), Duke University Medical Center, Durham, North Carolina 27710; the Receptor Biology Section (J.F.C., K.S.K.), Laboratory of Reproductive and Developmental Toxicology, National Institute of Environmental Health Sciences, National Institutes of Health, Research Triangle Park, North Carolina 27709-2233; Departments of Biochemistry and Child Health (D.B.L.), University of Missouri, Columbia, Missouri 65211; the Departments of Biochemistry, Molecular and Cell Biology (A.M., K.E.M.), Northwestern University, Evanston, Illinois 60208-0835; and the Chemical Industry Institute of Toxicology (M.S.), Research Triangle Park, North Carolina 27709-2137

ABSTRACT

Targeted disruption of the mouse estrogen receptor-α gene (estrogen receptor-α knockout; ERKO) results in a highly novel ovarian phenotype in the adult. The ERKO mouse model was used to characterize ERα-dependent processes in the ovary. Visualization of the ovaries of 10-, 20-, and 50-day-old wild-type (WT) and ERKO mice showed that the ERKO phenotype developed between 20 and 50 days of age. Developmental progression through the primordial, primary, and antral follicle stages appeared normal, but functional maturation of preovulatory follicles was arrested resulting in atresia or in anovulatory follicles, which in many cases formed large, hemorrhagic cysts. Corpora lutea were absent, which also indicates that the normal biochemical and mechanical processes that accomplish ovulation were compromised.

Northern and ribonuclease protection analyses indicated that ERKO ovary FSH receptor (FSHR) messenger RNA (mRNA) expression was approximately 4-fold greater than in WT controls. Ovarian LH receptor (LHR) mRNA expression was also higher in the ERKO animals. Cellular localization studies by *in situ* hybridization analysis of ERKO ovaries showed a high level of LHR mRNA expression in the granulosa and thecal layers of virtually all the antral follicles. Ribonuclease protection analyses showed that ovarian progesterone receptor and androgen receptor mRNA expression were similar in the two groups. These results indicated that ERα action was not a prerequisite for LHR mRNA expression by thecal or granulosa cells or for ovarian expression of progesterone receptor mRNA.

Ovarian estrogen receptor β (ERβ) was detected immunohistochemically, was sharply compartmentalized to the granulosa cells, and was expressed approximately equally in the ERKO animals and the WT controls. In contrast, ERα staining was present in the thecal cells but not the granulosa cells of the WT animals.

The summary findings indicate that in the adult the major cause of the ERKO phenotype is high circulating LH interacting with functional LHR of the theca and granulosa cells. These features result in a failure of the normal maturational events leading to successful ovulation and luteinization and presumably involve both hypothalamic-pituitary and intraovarian mechanisms dependent upon ERα action. The presence of ERβ in the granulosa cells did not rescue the phenotype of the ovary. (*Endocrinology* **140:** 2733–2744, 1999)

ESTROGEN ACTION IS clearly responsible for full expression of the female phenotype. Classical studies established that the action of estrogen was receptor-mediated and also demonstrated the presence of estrogen receptor (ER) protein in cells of the major target organs and glands necessary for reproduction, *i.e.* hypothalamus, anterior pituitary, mammary gland, uterus, and ovary (1). Relative to other organs, however, the role of estrogen and its receptor-mediated actions in the ovary are much less well understood. Experimentally, this has been due to the difficulty of blocking estrogen synthesis definitively or in assessing accurately the pharmacological efficacy of estrogen agonists or antagonists in competition with the large amounts of locally synthesized endogenous ligand. Ovarian ER is expressed primarily by the granulosa cells associated with follicular growth. When follicle growth is terminated by luteinization or atresia, the level of ER expression by granulosa cells compared with the rest of the ovary is approximately equal (2). The level of expression may vary with species (3). Ovarian ER action is presumably involved in those processes demonstrated to be estrogen-dependent *in vivo*, *e.g.* mitosis and growth factor expression (4, 5), apoptosis (6), gap junctional area and integrity (7), and the modulation of FSH receptor (FSHR) and LH receptor (LHR) expression (8).

The principal extra-ovarian sites of estrogen action critical to ovarian function involve cells of the hypothalamus and anterior pituitary that regulate gonadotropin secretion. ER-mediated regulation at this level was demonstrated in adult mice in which ERα gene disruption (estrogen receptor-α knockout; ERKOs) resulted in increased steady-state FSHβ and LHβ mRNA expression and elevated circulating LH levels (9, 10), indicating a disruption in the negative feedback

Received November 16, 1998.

Address all correspondence and requests for reprints to: Dr. Kenneth Korach, NIH-NIEHS, P.O. Box 12233/111 Alexander Drive, Research Triangle Park, North Carolina 27709-2233. E-mail: korach@niehs.nih.gov.

* Supported in part by grants HD-11827 (D.W.S.), HD-21921 (to K.E.M.), and P30 Center HD-28048 (to K.E.M.) from the NICHD, NIH.

response. In adult ERKOs, preovulatory follicle development is altered, and, rather than progressing to ovulation, culminates in many cases in the formation of large, cystic, and hemorrhagic follicles (11). Extended treatments with the estrogen antagonists such as ZM 189,154 and EM-800 (12–14) also produce changes in hypothalamo-pituitary and ovarian function similar to those obtained with ERα gene disruption. However, their effects can vary significantly with dose and do not specifically designate the actions of the ERα or of ERβ, a new, recently cloned separate ER form (15). Also, as pointed out above, it is difficult to know the extent to which local follicular estrogen production modulates ovarian cellular responses to these agents.

The ERKO mouse model previously described provides a more direct experimental approach by which to characterize the intraovarian processes dependent upon ERα and, simultaneously, to indicate mechanisms that might be dependent upon ERβ. ERβ mRNA is highly expressed in the granulosa cells of the rat ovarian follicle (16) and is normally expressed in the ovaries of ERαKO mice (17). The working hypotheses we tested with this model in this study were: 1) that LHR expression in granulosa cells requires ERα action, 2) whether expression of progesterone receptor (PR) in the ovary requires ERα action, and 3) whether, in addition to ERβ mRNA, ERβ protein is actually expressed in the ovary.

Materials and Methods

ERKO mice and superovulation regime

The ER gene was disrupted as described previously using homologous recombination gene targeting to create mice lacking a functional ERα. The breeding, genotyping, and daily care of the mice have been described (11, 18). All procedures involving animals were approved under an NIEHS Animal Care and Use protocol and were performed in accordance with USPHS guidelines. Five or six 15- to 16-week-old animals of each genotype were injected sc with a single dose of 2.2 IU PMSG (Sigma Chemical Co.) at 1300–1400 h followed by 3.2 IU human CG (hCG) (Sigma Chemical Co.) 48–52 h later. This dose of gonadotropin is the routine protocol used at NIEHS. Animals were killed 20–24 h after the hCG injection, and the ovaries trimmed and processed histologically.

Histological preparation

Ovaries for routine histological analysis were placed into 10% buffered formalin at 4 C for a period of 6–18 h, followed by transfer to 70% ethanol. The tissue was then imbedded in paraffin, sectioned, and stained with hematoxylin and eosin according to standard histological procedures or used for immunohistochemical analysis as described below.

Gonadotropin and steroid receptor mRNA analysis

Generation of riboprobes. All riboprobes used were generated from linearized templates using Maxiscript reagents with the appropriate RNA polymerase (Ambion, Inc., Austin, TX), and the incorporation of [^{32}P]-CTP (Amersham Life Sciences, Arlington Heights, IL). The antisense riboprobe for the mouse PR mRNA corresponded to bp 2417–2781 of the mouse PR complementary DNA (cDNA) (GenBank accession no. M68915). This was generated from a subclone (bp 1672–2781) of the mouse PR cDNA in pBluescript KS- (Stratagene Cloning Systems, La Jolla, CA), kindly provided by Dr. Vicki Davis, that was first linearized with the internal *Eco*RI site (at bp 2417) and then transcribed with T3 RNA polymerase. The riboprobe for the mouse androgen receptor (AR) mRNA was generated from a subclone of bp 2379–2817 of the mouse AR cDNA (GenBank accession no. X53779) in pBluescript SK- (Stratagene), kindly provided by Dr. Jonathan Lindzey. The mAR antisense riboprobe was generated from a template linearized with *Eco*RI and then transcribed with T3 RNA polymerase. To allow for normalization of the amounts of total RNA loaded per lane on a Northern blot, an antisense riboprobe for the mRNA of the mouse ribosomal protein L-7 (bp 371–639; GenBank accession no. M29016) was used. To allow for normalization between samples in the RNase protection assay (RPA), an antisense riboprobe for the mouse cyclophilin mRNA was generated from the template pTRI-Cyc (Ambion, Inc.) and used.

The generation of labeled antisense riboprobes for the mouse FSHR and LHR first required cloning of the coding sequences into a suitable vector. This was carried out by RT-PCR amplification of partial cDNA sequences of the FSHR and LHR from wild-type (WT) mouse ovarian RNA. The following primers targeting the extracellular domains of each receptor were used: for FSHR, 525-bp fragment (bp 128–652 of rat cDNA; GenBank accession no. LO2842): forward 5′-CACTGGCTGTGTCATTGCTCT-3′ to reverse 5′-CTGAGTTCCGTTGAATGCACA-3′; for LHR, 505-bp fragment (bp 256–760 of rat cDNA; GenBank accession no. M81310) forward 5′-TCTCTCAGAGTGATTCCCTG-3′ to reverse 5′-AGCGTCTGAATGGACTCCAG-3′. Reverse transcriptase generation of cDNA was performed on 0.4 μg of poly A RNA using the GeneAmp RNA PCR kit (Perkin Elmer Corp., Norwalk, CT) with random hexamers according to the manufacturer's protocol except that all reagents were scaled up to 50 μl per reaction. PCR was carried out using 3.0 μl of the reverse-transcriptase-generated cDNA per reaction with the appropriate primers at 100 pmol each, dinucleotide triphosphates at 0.2 mM each, 2.5 U AmpliTaq DNA polymerase (Perkin Elmer Corp.) and the corresponding optimal buffer (LHR, Buffer N; FSHR, Buffer A) (Invitrogen Corp., San Diego, CA) at 1× in a total volume of 50 μl. Thermal cycling was carried out at 95 C/30 sec; 58 C/1.0 min; 72 C/1.0 min for 35 cycles in a GeneAmp 9600 (Perkin Elmer Corp.). The amplified sequences were then cloned into the Srf 1 site of PCR-Script (SK(+) (Stratagene, La Jolla, CA) according to the manufacturer's protocol. Antisense riboprobes were generated from linearized templates using the appropriate RNA polymerase, T7 for LHR and T3 for FSHR.

Northern blot analysis

Total RNA was extracted from pooled ovarian tissue (1.7 g) from adult WT adult females and from pooled ovarian tissue (2.9 g) from adult ERKO females using TRIZOL reagent (Gibco BRL, Gaithersburg, MD) according to the manufacturer's protocol. Final yield was quantified by UV spectrophotometry, and the RNA was checked for integrity on a 1% agarose gel. Duplicate 20 μg fractions of total RNA from each genotype were electrophoresed on a 1.5% agarose/1× MESA (MOPS-EDTA-sodium acetate) buffer/6.7% formaldehyde gel system. The gel was blotted to Hybond N nylon (Amersham Life Science, Arlington Heights, IL) by salt capillary transfer according to the manufacturer's instructions. The resulting membrane was crosslinked using a UV cross-linker (Stratagene Cloning Systems, La Jolla, CA). The blot was then halved and each half probed for either the FSHR or LHR mRNAs. Prehybridization consisted of 6–8 h in a Hybaid oven at 65 C in 50% formamide, 3 × SSC, 5 × Denhardt's, 0.02 M $NaPO_4$, 10% dextran solution, and 1% SDS. For each antisense riboprobe, 3 × 10^6 cpm/ml was added and allowed to hybridize overnight at 65 C. The membranes were then washed 2 × 15 min in 2× SSC/0.1% SDS at room temperature followed by 2 × 14 min in 0.1× SSC/0.1% SDS at room temperature followed by 2 × 15 min in 0.1× SSC/0.1% SDS at 68 C. The resulting bands were visualized and quantified with the Phosphorimager 425 and accompanying ImageQuant Software (Molecular Dynamics, Inc., Sunnyvale, CA) followed by exposure to x-ray film.

RNase protection assay

Assays were carried out on 2.5 μg total ovarian RNA from individual adult WT and ERKO females using the Hybspeed RPA kit (Ambion, Inc.) according to the manufacturer's protocol. Assays for each particular mRNA were carried out in separate tubes (except for those for the FSHR and LHR mRNAs) containing target RNA and 1 × 10^5 cpm each of the respective antisense riboprobe and the antisense mouse cyclophilin riboprobe. Protected fragments were separated on a 6% bis-acrylamide/8.3 M urea/1 × TBE gel (National Diagnostics Systems, Atlanta, GA). Each antisense riboprobe produced the following size-protected fragments: AR = 439 nt, Cyc = 103 nt, FSHR = 355 nt, LHR = 236 nt, and PR = 365 nt. Note that the antisense riboprobes for the FSHR and LHR

mRNAs were shortened to produce protected fragments of sizes that were more optimum to the RPA. The gels were then fixed and dried using the Hoeffer Easy Breeze gel drying system. The resulting bands were visualized and quantified with the Storm 850 Phosphorimager and accompanying ImageQuant software (Molecular Dynamics, Inc., Sunnyvale, CA) followed by exposure to x-ray film.

Antibodies and immunocytochemistry

A rabbit polyclonal antibody (PAI-310) raised against a synthetic peptide corresponding to the C-terminal amino acid residues 467–485 of rat ERβ was purchased from Affinity BioReagents, Inc. (Golden, CO). The characterization of this antibody by Western blot and gel supershift was accomplished using rat ERβ overexpressed by COS-7 cells. ERα monoclonal antibody (clone 1D5; DAKO Corp., Carpinteria, CA) binds to estrogen receptors and localizes ERα in target tissues both by immunofluorescence and immunoperoxidase (19).

The paraffin sections were first deparaffinized and then treated with 3% H_2O_2 in PBS (pH 7.6) for 5 min. These steps were followed by heating the sections in a microwave oven (3–4 min each) for antigen retrieval using a citrate buffer pH 5.5–5.7 (HIER buffer, 1:10 dilution, Ventana Medical Systems, Inc., Santa Barbara, CA) and processed for immunostaining by the avidin-biotin peroxidase method as previously described (20). The sections were incubated overnight at 4 C with ERβ antibody, preadsorbed ERβ antibody or ERα monoclonal antibody, (ID5, DAKO Corp.). ERβ antibody was used at a concentration of 5 μg/ml and ID5 monoclonal antibody at a concentration of 0.1–0.2 μg/ml. Sections were washed in 1.0 mM PBS (pH 7.6) followed by incubation with the secondary antibody, goat-antirabbit IgG or horse-antimouse IgG, and Elite avidin-biotin peroxidase at a concentration of either 1:100 or 1:200 for 30 min each at room temperature. After a 5-min wash, the sections were treated with liquid diaminobenzadine (DAB) (BioGenex Laboratories, Inc., San Ramon, CA) followed by a 10-min wash in PBS and then counterstained with hematoxylin. Specificity of the ERβ antibody was established by incubating the sections either with normal rabbit serum or preadsorbed ERβ antibody, prepared by incubating 5.0 μg of ERβ antibody with 20 μg peptide in 1.0 ml for 24 h at 4 C. The specificity of ERα immunostaining was established by incubating sections of ovary and oviduct with the normal mouse IgG, which did not show specific immunoreaction.

In situ hybridization

Twenty-micrometer sections of fresh-frozen ERKO and WT ovaries were prepared using a Reichert 820 cryostat (Buffalo, NY) and mounted onto gelatin and poly-L-lysine-coated glass slides for *in situ* hybridization as described previously (21). Hybridization probes used were [^{35}S]-UTP-labeled riboprobes derived from a rat LH-receptor cDNA subclone. Hybridization was continued for 12–18 h at 47 C in a humidified chamber. Sense riboprobes were used as controls. Subsequently, the slides were washed to a final stringency of 0.2× SSC at 55 C after a 1-h treatment with 20 μg/ml RNase at 37 C. Slides were then processed for emulsion autoradiography (NTB-2, Eastman Kodak Co., Rochester, NY). Exposure time on emulsion was 2 weeks. After development, slides were stained with hematoxylin to visualize nuclei. The sections were then examined and photographed using a macroscope (Wild M420, Leica Corp., Heerbrugg, Switzerland) or a microscope (Nikon Optiphot, Nippon Kogaku [USA] Inc., Garden City, NY).

Histochemical detection of apoptosis

Ovaries from adult WT and ERKO females were removed and fixed in 4% paraformaldehyde (pH 7.0) for 4–6 h at 4 C. The tissues were then transferred to 70% ethanol at 4 C for 24 h, embedded in paraffin, and sectioned at 5 microns. Sections were mounted on silanized slides (Oncor, Gaithersburg, MD) and processed through the MEBSTAIN Apoptosis Kit (Medical & Biological Laboratories, Watertown, MA) according to the manufacturer's protocol. This kit utilizes a fluorescent label and is based on the TUNEL method. A single modification was made where the incubation time during the proteinase K step was increased from 30 m to 1 h. Stained sections were coverslipped using Antifade reagent (Oncor) as a mounting medium to maintain the fluorescent signal as long as possible. Sections were evaluated and photographed using a Zeiss Photomicroscope and Fugi Provia 1600 film at ASA 800 (Carl Zeiss, Thornwood, NY).

Results

Ovarian development

Our initial studies characterizing the phenotypic effects of ERα gene disruption were restricted to adult animals. We evaluated whether the adult phenotype observed earlier (11) was developmentally determined or a result of aging. Neonatal ERKO females have ovaries which are indistinguishable from those of WT females from a gross morphological standpoint, and which at 10 days of age contain histologically normal primordial and primary follicles (Fig. 1, A and B, WT ovaries; E and F, ERKO ovaries). At 20 days, the ovarian phenotype of the ERKO animals changes slightly. The ovaries contain some follicles that have developed to the antral stage (Fig. 1, C and D, WT ovaries; G and H, ERKO ovaries), perhaps secondary to an elevation in gonadotropin levels, first noticeable in ERKO animals at about this time (10). The ovarian phenotype in 50-day, postpubescent, ERKO animals is very similar to the initial description in older (12 week), acyclic adult animals (11, 22). Follicle development in the ERKO animals culminates in atresia or as hemorrhagic cysts, whereas corpora lutea, representative of successful ovulation in response to appropriately timed gonadotropin surges, are present in the WT ovary and not in the ERKO (compare Fig. 2A and 2B). The absence of corpora lutea is not conclusive evidence of anovulation but is highly correlative. To date, we have not observed corpora lutea in any of the sections analyzed. Figure 2C (*arrow*) shows a high-power view of a hemorrhagic, cystic follicle in which only a single granulosa cell layer remains. Adjacent antral follicles contain several granulosa cell layers, indicative of an initial, functional follicular growth response to gonadotropin. Figure 2D shows a thecal blood vessel of a PMSG-stimulated ovary hemorrhaging into the follicular antrum. Hemorrhage into the follicles can occur at multiple points and also occurs before death of all the granulosa cell layers (not shown). We attempted to induce ovulation in adult ERKO mice in the absence of a GnRH antagonist. Exogenous PMSG followed by hCG treatment of adult animals did not result in ovulation as indicated by the absence of corpora lutea. The thecal layer of these follicles was hypertrophied. The granulosa cells tended to dissociate from each other and from the lamina propria suggesting a lack of cell-to-cell association in this compartment (not shown).

Ovarian gonadotropin receptor mRNA expression

The 2.6-kb FSH mRNA transcript detected in ovaries of both WT and ERKOs (Fig. 3) corresponds to the most abundant transcript previously described in both rat testis and granulosa cells (23, 24). Similarly, several LHR mRNA transcripts correspond to those previously described for rat ovary, mouse testis, and mouse MA-10 Leydig cells (25). These results validate the accuracy and specificity of the probes. When RNA pooled from several trimmed ovaries of each genotype were compared by Northern analysis, the FSHR and LHR transcripts representing the ERKO were appreciably elevated compared with the WT

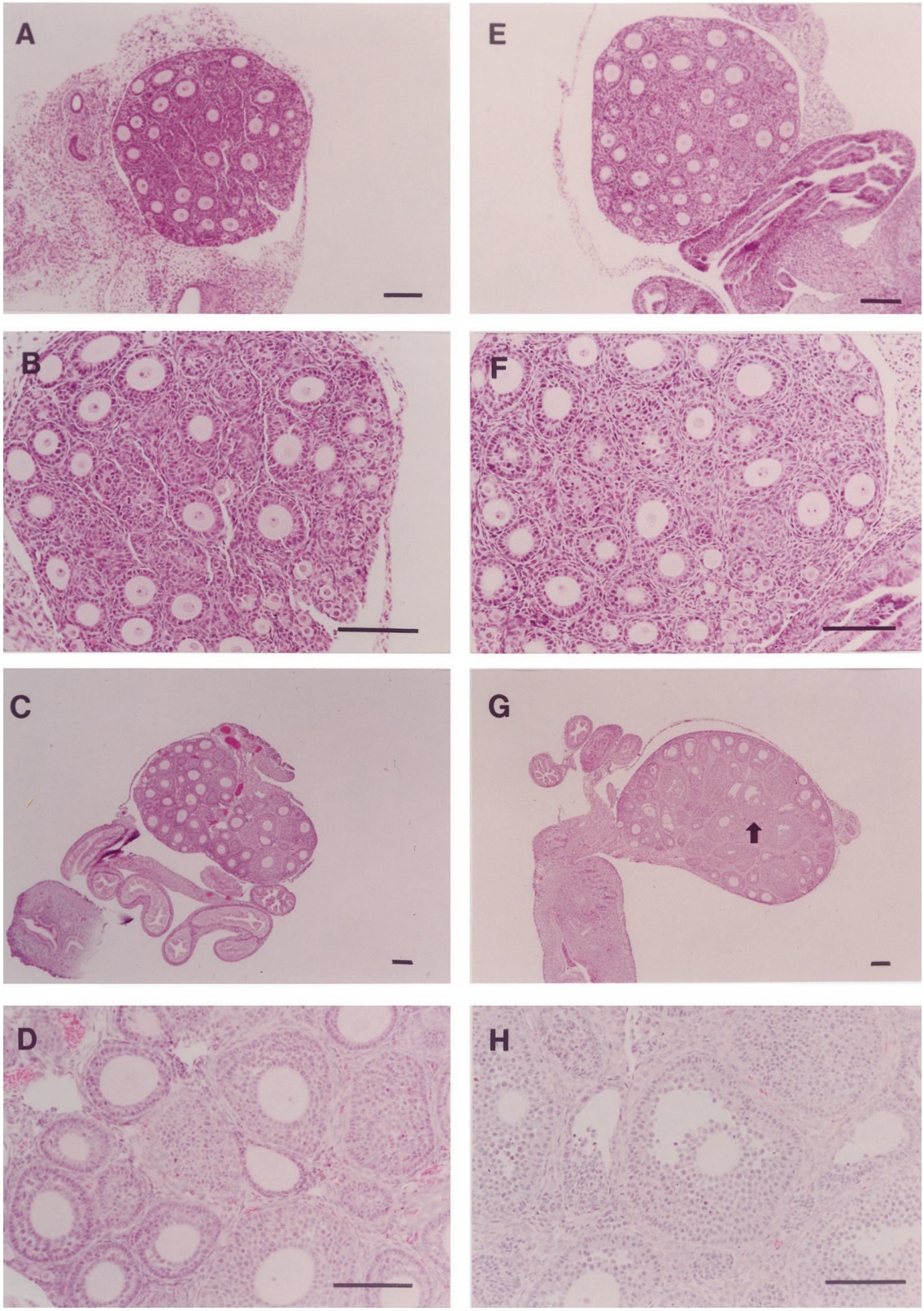

FIG. 1. Prepubertal ovarian phenotype in the ERKO mouse. A (25×) and B (50×), Representative WT ovary at 10 days of age, demonstrating the presence of primordial and primary follicles. C (10×) and D (50×), WT ovary at 20 days of age, demonstrating the growth of some follicles to a secondary or preantral stage. E (25×) and F (50×), Representative ERKO ovary at 10 days of age which appears similar to the WT. G (10×) and H (50×), Representative ERKO ovary at 20 days containing several preantral follicles as well as some early antral follicles (indicated by *arrow*). At 20 days, a distinguishing phenotype may be first becoming apparent in the ERKO ovary in the form of premature stimulation of follicular growth as evidenced by antral follicles. *Scale bars*, 1 mm. Hematoxylin and eosin (H&E) staining.

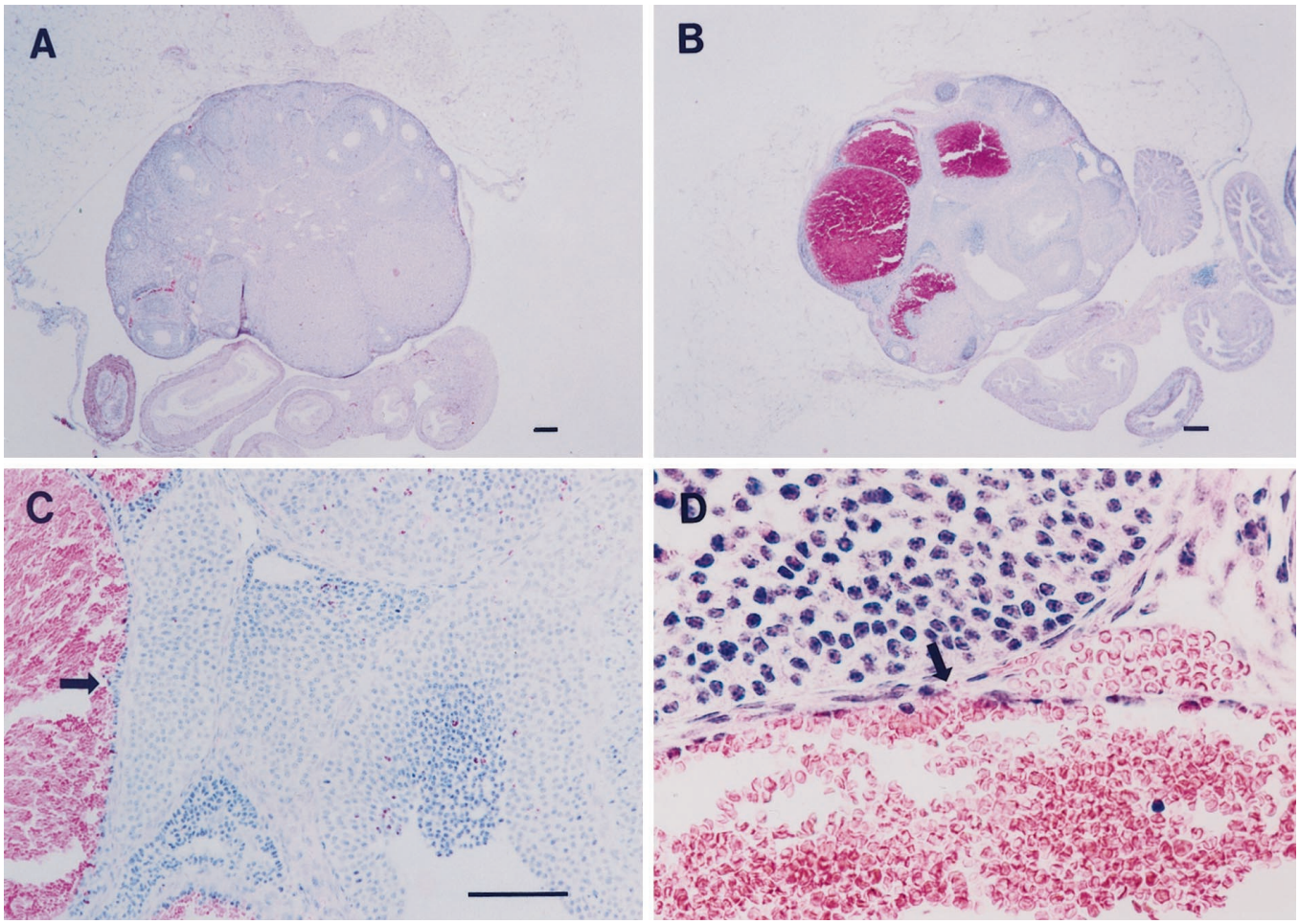

FIG. 2. Adult ovarian phenotype in the ERKO mouse. The WT ovary (A, 40×) is representative of that in normally cycling adult mice and demonstrates follicles at various stages of maturation and at least two prominent corpora lutea. The ERKO ovary (B, 40×; C, 200×) is representative of an adult ERKO ovary, demonstrating preantral and antral follicles, some of which eventually develop into the large hemorrhagic cystic follicles shown. No corpora lutea have been observed in the ovaries of adult ERKO mice, indicating a lack of spontaneous ovulation. C, High power view of the ovary shown in panel B and shows regression of the granulosa cell layers, presumably secondary to apoptosis, in the hemorrhagic follicle. Adjacent follicles contain several granulosa cell layers. D (200×), Thecal vessel of an PMSG-stimulated ERKO ovary hemorrhaging into the follicular antrum (*arrow*).

ovary. Figure 4A demonstrates expression of the most abundant FSHR and LHR mRNA transcripts when analyzed in individual WT and ERKO ovarian samples by RNase protection assay. In agreement with the Northern, ERKO ovary FSHR mRNA expression averaged approximately 4-fold higher than WT controls. Average LHR mRNA expression was slightly higher in the ERKO ovaries (Fig. 4B). Because factors such as the number of preovulatory follicles and corpora lutea can introduce variability and complicate the interpretation of LHR mRNA expression on the basis of whole-ovary mRNA levels in these type comparisons, we performed *in situ* hybridization analyses of LHR mRNA expression.

In situ hybridization

In the hypophysectomized rat model, the combined action of estradiol and FSH potentiated FSH-dependent FSHR binding. Furthermore, FSH and estradiol were essential for optimal induction of granulosa cell LHR mRNA expression and membrane receptor binding (8). The combination of the ERKO model with an *in situ* hybridization approach allows a determination as to whether these fundamental steps in granulosa cell differentiation are dependent upon ERα–mediated actions. *In situ* FSHR expression was marginally above background and was not sufficiently definitive (not shown). Figure 5 (*top panel*) indicates the specificity of the LHR probe used in all of the studies: the sense probe produced only a very low background. The antisense probe detected LHR mRNA in specific ovarian cell types in PMSG-stimulated WT and ERKO ovaries. The representative WT ovary shows LHR mRNA expression by the granulosa and thecal layers of the follicle as well as the interstitium and the corpus luteum (Fig. 5; antisense; *middle panels*). The representative ERKO ovary shows high-level LHR mRNA expression in the granulosa and thecal compartments of virtually all of the large antral follicles present (Fig. 5; antisense; *lower panels*). These results indicate that ERα action is not required for LHR mRNA expression by interstitial, thecal, or granulosa cells.

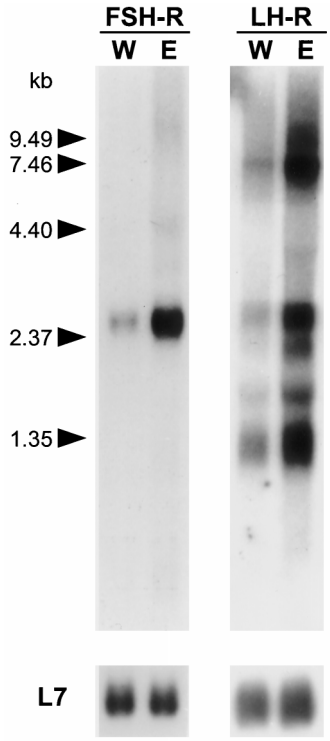

FIG. 3. Northern blot analysis for mRNA encoding the FSHR and the LHR in pooled WT and pooled ERKO ovaries. Duplicate blots of 20 μg total RNA from pooled WT (W) and pooled ERKO ovaries (E) were generated as described in *Materials and Methods*. They were then probed with ^{32}P-labeled riboprobes specific for the mouse FSHR mRNA or the mouse LHR mRNA and then stripped and reprobed for the mRNA encoding the ribosomal protein L7 mRNA for normalization purposes. Note the significantly increased levels of the single FSHR transcript as well as the multiple LHR transcripts in the ovaries of the ERKO mice compared with that of their WT counterparts.

ERβ protein localization

Because ERβ mRNA is expressed in the WT and ERKO mouse ovary and by the granulosa cells of WT rats (16, 17), we analyzed adult ovaries of WT and ERKO animals for ERβ protein localization by immunohistochemistry. Figure 6, A and C, shows low and high power views, respectively, of ovarian ERβ localization in WT ovaries. The principal feature is pronounced granulosa cell nuclear staining. Some staining is also evident in precorona radiata and precumulus cells immediately surrounding the oocyte. Theca interna cells did not express detectable ERβ protein. All ovarian cell types stained at background levels in sections preabsorbed with peptide (low and high power views, Fig. 6, B and D, respectively). Ovarian ERβ staining in the ERKO animals was essentially the same as that of WT controls, showing pronounced expression by granulosa cells and the cell types immediately surrounding the ovum (Fig. 6, E and F, low and high power, respectively). In contrast, ERα protein was absent in the granulosa compartment of comparable follicles in the WT animals but was expressed by thecal and interstitial cells (Fig. 6G). Nuclear staining was absent in sections processed without primary antibody, indicating specificity of the antibody (Fig. 6H).

Apoptosis in antral follicles

A characteristic feature of the ERKO ovarian phenotype is that of follicle development to the large antral stage but with a lack of progression to final maturation culminating in ovulation. Figure 7A is a representative example of a mature antral follicle with several granulosa layers, a morphology compatible with that of a preovulatory follicle. However, many granulosa cells are undergoing apoptosis as indicated by nuclear pycnosis, those sloughed into the follicular antrum have undergone lysis, and the oocyte is degenerating. Beyond this stage, the surviving follicles become cystic. Figure 7B shows by another procedure, fluorescence TUNEL methodology, that the granulosa cells of ERKO follicles undergo apoptosis. The incidence of granulosa cell apoptosis was comparable in both genotypes (data not shown), suggesting that the process is not principally dependent upon ERα.

Ovarian steroid receptor mRNA expression

The other two major sex steroid receptors, PR and AR, are also expressed by granulosa cells (8, 21). Since induction of at least some forms of PR depends upon functional estrogen receptor (18), it was of interest to know whether ovarian PR mRNA is expressed by the ERKO genotype. Also, AR levels could be hypothesized to be different in ERKO animals because their serum levels of testosterone are elevated about 10-fold (26). Accordingly, we also compared ovarian AR mRNA expression in WT and ERKO animals. The steady-state levels of AR and of PR mRNA were the same in both genotypes (Fig. 8). Therefore, the anovulatory ERKO phenotype is not associated with marked differences in steady-state ovarian PR and/or AR gene expression.

Discussion

This study and others from our laboratory have now established that ERα disruption results in altered developmental ovarian morphology, enhanced androgen, estrogen, and LH secretion, elevated FSHR mRNA expression, and the formation of cystic, hemorrhagic follicles in association with anovulation. ERα disruption did not inhibit formation of the ovary itself or of the oocyte, did not alter circulating serum FSH levels, and did not prevent LHR, AR, PR mRNA expression, or ERβ protein expression.

Because ER plays such a crucial role in female reproductive development, it was not unreasonable to expect that ERα disruption might produce a phenotype lacking ovaries or one severely depleted of oocytes at an early developmental stage. This was not the case. Oocytes were present and biochemically functional in the sense that they contributed to granulosa cell and follicle formation. This implies that ERα action is not essential for the functional activity of at least one oocyte-derived growth factor because disruption of the oocyte factor GDF-9 gene leads to premature demise of ovarian follicles at the one-layer granulosa cell stage of primary follicle development (27). ERα disruption was compatible with apparently normal follicle development up to 10 days after birth, with differences beginning to be evident at 20 days. The accelerated follicle development is probably secondary to

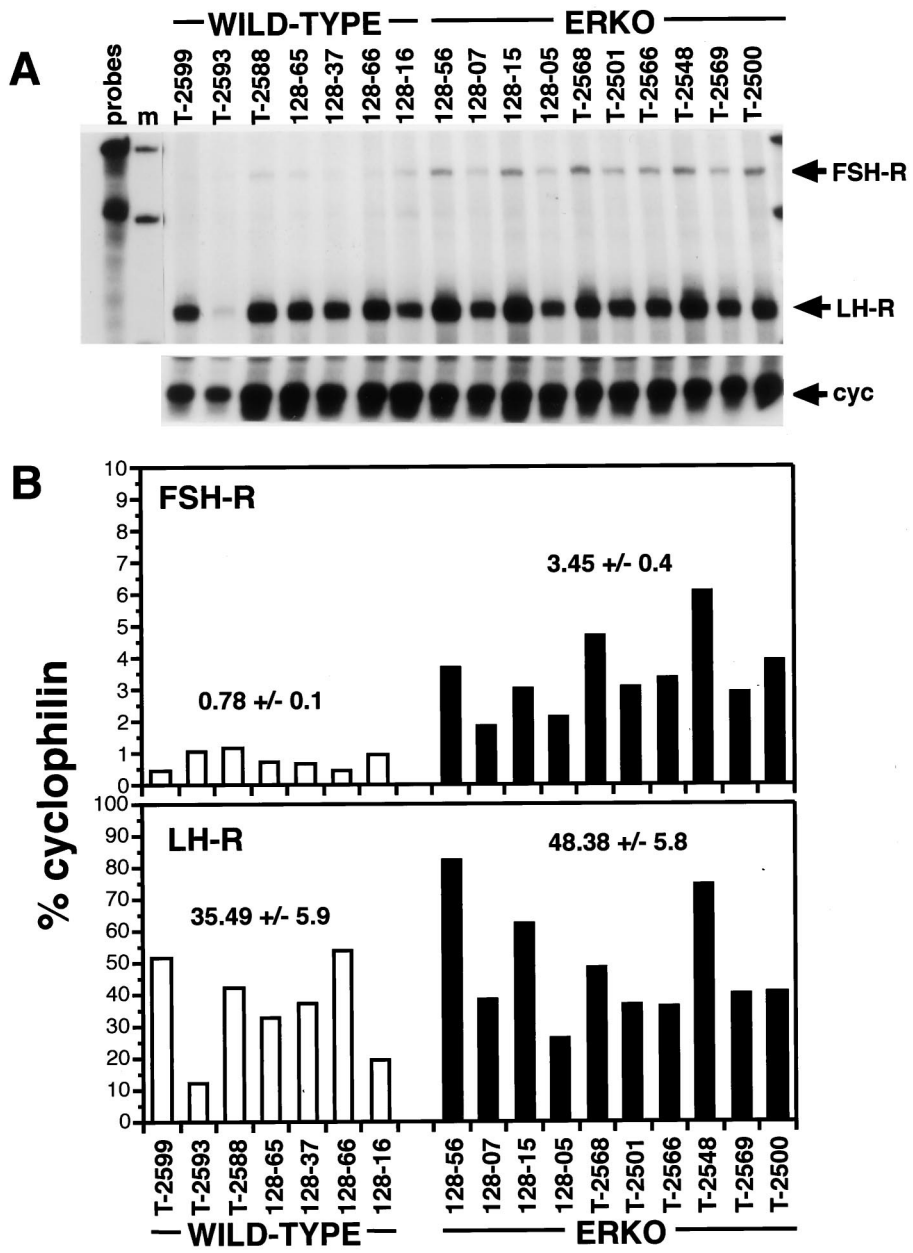

FIG. 4. RNase protection assay for mRNA encoding the FSHR and LHR in individual WT and ERKO ovaries. Total ovarian RNA (2.5 μg) from individual WT and ERKO females was assayed as described in the *Materials and Methods*. A riboprobe for cyclophilin mRNA (cyc) was included in each assay for normalization purposes. B, Quantitative analysis of the data shown in panel A, indicating that the levels of mRNA for both the FSHR and the LHR are elevated in ovarian tissue from individual ERKO females compared with their age-matched counterparts. Printed above each set of graphs are the relative average levels (± SEM) of the transcripts for each genotype.

elevated gonadotropin levels, first observable at about this time. In postpubertal-age animals, antral follicles developed and were steroidogenically active in terms of androgen and estrogen secretion (26) but did not progress to ovulation. The mechanisms contributing to anovulation presumably are responsible in part for the dramatic finding of large, cystic, hemorrhagic follicles in the ERKO animals (11).

Other genetic models, such as the gene disruptions of FSHβ, insulin-like growth factor I, cyclin D2, COX-2, PR, and vitamin D exemplify follicular arrest at various developmental stages (28–32). Follicular development in the FSHβ and insulin-like growth factor I knockout models progressed only to the early antral stage. In the majority of cases, follicle development in mice overexpressing Follistatin arrests between the primary and antral follicle stages (33). Development in the cyclin D2-knockout animals progressed only to follicles with four granulosa cell layers, and COX-2 knockout animals developed ovulatory follicles that luteinized and formed corpora lutea but failed to release the ovum. Ovaries of aromatase knockouts develop follicles with numerous granulosa cells but fail to ovulate; those of Connexin 37 knockouts do not develop Graafian follicles and also fail to ovulate (34, 35). PR knockout animals formed preovulatory follicles that failed to ovulate (36). These models emphasize the complexity and interdependence of various systems having regulatory input to the processes of follicular development and ovulation. The now characteristic ERKO phenotype of cystic, hemorrhagic follicles did not develop in any of the above-described models.

A major contributory factor to the anovulatory and cystic, hemorrhagic follicular state(s) in the ERKO females seems to involve the physiological regulation of LH and its receptor.

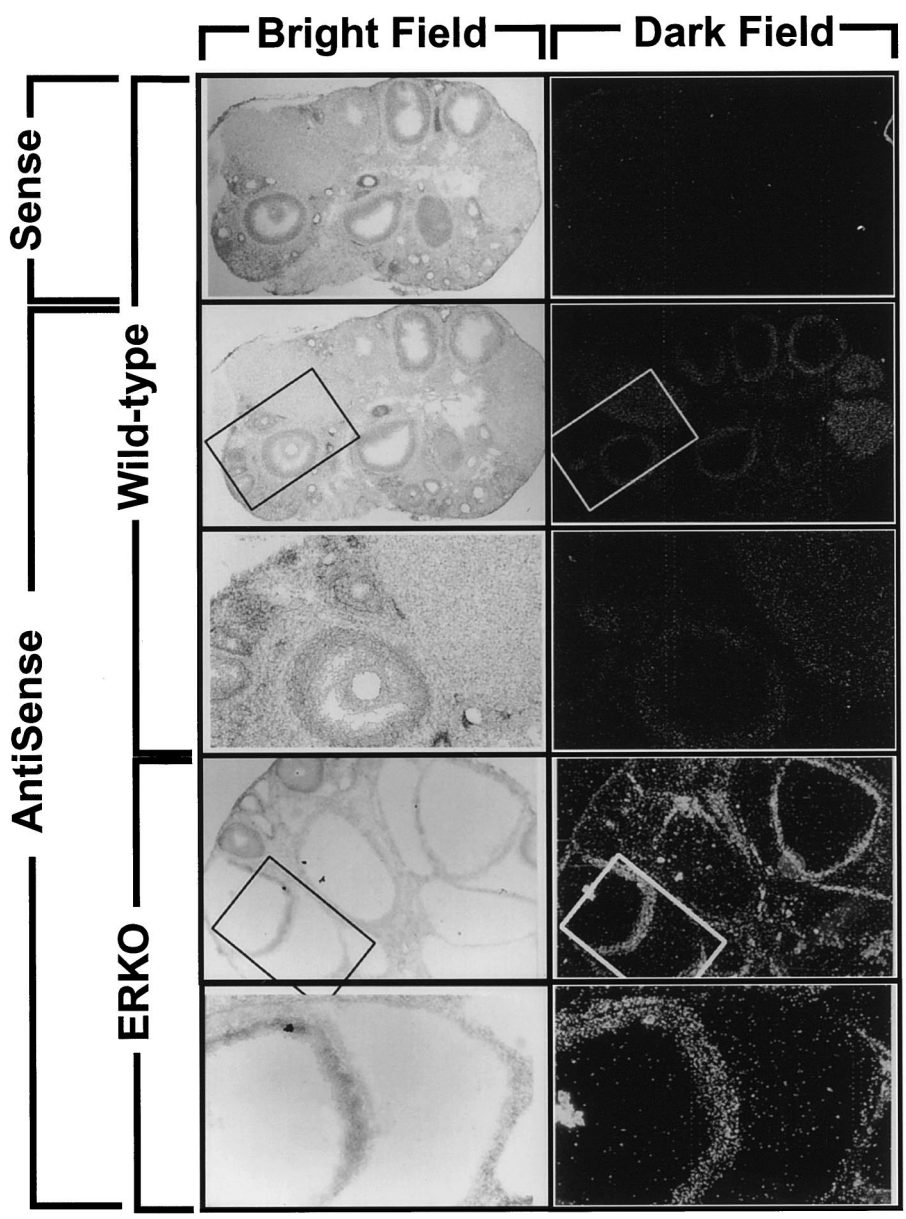

FIG. 5. Comparison of LHR mRNA expression in ERKO and WT ovaries by *in situ* hybridization. The panel represents photomicrographs of ovaries of WT and ERKO animals treated with PMSG for 48 h. Panels on the *left* show tissue histology, while panels on the *right* are photographs of the same field taken using darkfield optics to show the silver grains indicating the hybridization signal. The *top right panel* (Sense) shows a section probed with a sense cRNA probe to serve as a control for hybridization specificity (40× magnification). The remaining panels show sections probed with an antisense cRNA probe (Antisense) at different magnifications (40×, *upper*; 100×, *lower*, the rectangular boxed area of the 40× magnification) for both WT and ERKO ovaries. The WT ovaries express LHR mRNA within a few discreet structures, the larger follicles and early corpora lutea. In contrast, the ERKO ovaries show widespread expression of LHR mRNA in almost all follicles. The large, cystic follicles with only a few granulosa cell layers remaining show a high level of LHR mRNA expression (ERKO antisense, *top panel*, 40× magnification). The large follicles in the *bottom panel* show high-level LHR mRNA expression by both the thecal and granulosa cell layers.

LH levels were significantly higher than in WT controls, but its secretory pattern was presumably acyclic because an estrogen-initiated response at the hypothalamic-pituitary level is necessary to elicit the ovulatory gonadotropin surge (37). The mouse pituitary expresses ERα, but levels of ERβ mRNA are low to absent (16, 38). Ovaries of the ERKO animals show biochemical and histological evidence of elevated LH stimulation: 1) circulating androgen levels are very high, and 2) thecal and interstitial cells are hypertrophied. The ovarian histological picture is quite similar to those of transgenic mice overexpressing bLHβ-CTP (39, 40). Both models exhibit normal follicular morphology in the early stages, but development then culminates in the formation of anovulatory, hemorrhagic, cystic follicles or granulosa cell tumors. Some corpora lutea develop in the bLHβ-CTP-overexpressing animals but are absent in the ERKO. This is one slight difference in ovarian morphology between the two models.

In situ analysis of LHR mRNA expression corroborated the histological picture. LHR mRNA expression was at a high level throughout the ovary and was more consistent among ERKO animals because of a relatively greater number of large antral follicles. There was considerable variability in LHR mRNA expression in the WT ovaries, which contained fewer large follicles of comparable size to those of the ERKOs, presumably because the WT animals better reflected the distribution of follicular development over the normal stages of the estrous cycle. A large proportion of signal was localized in the granulosa compartment. This is important because previous work established convincingly that estrogen action along with that of FSH was necessary to induce granulosa cell LHR binding and mRNA expression in the rat granulosa cell (8). Our combined RPA and *in situ* results show that ERα action is not necessary to achieve granulosa cell LHR mRNA expression in either the granulosa or the thecal compartment.

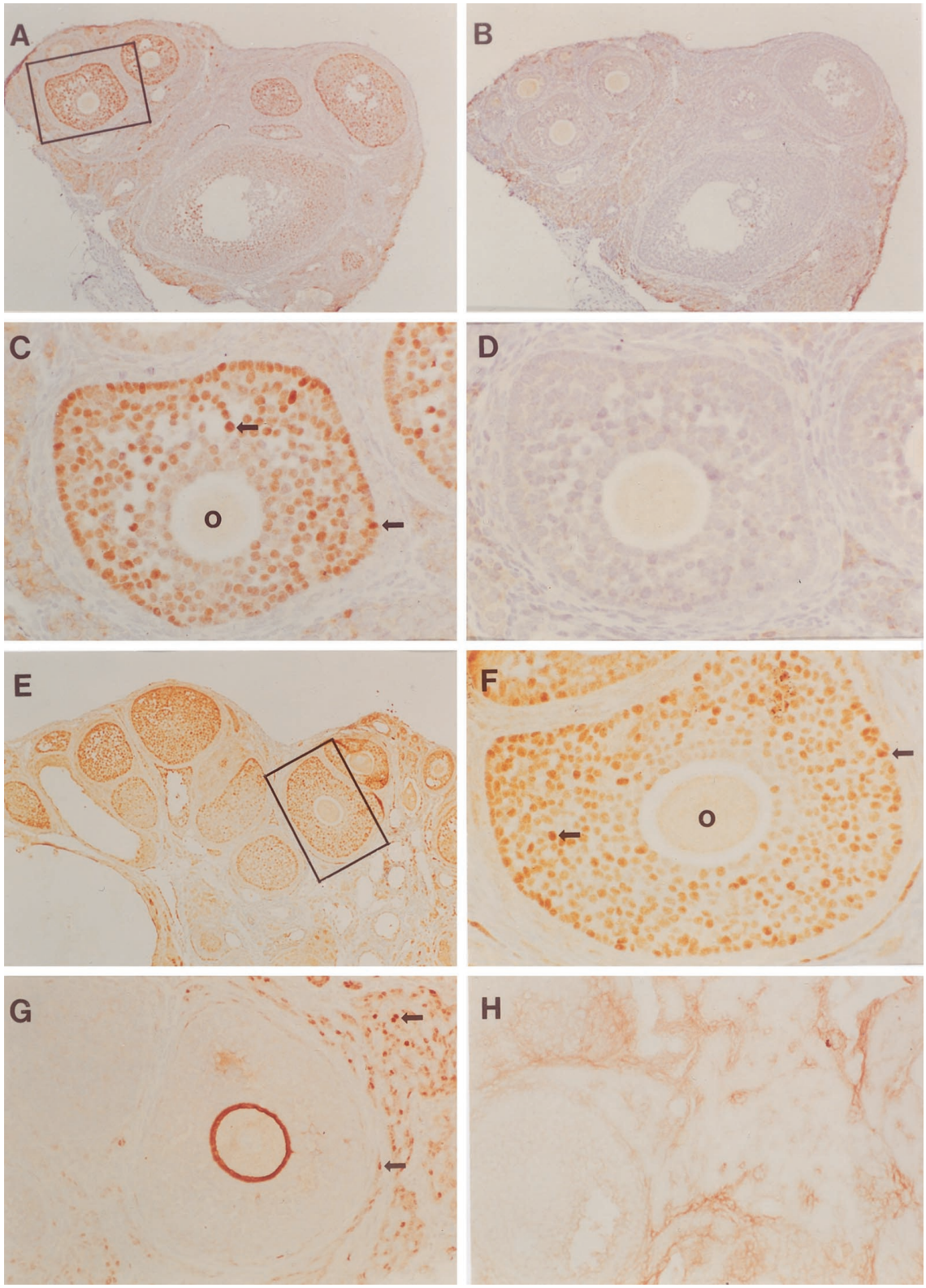

FIG. 6. Comparison of ERβ and ERα localization in ERKO and WT ovaries by immunochemistry. Ovaries were stained with ERβ antibody and secondary antibody as described *in Materials and Methods*. Prominent nuclear ERβ staining is evident in 40× and 100× magnification of sections of WT ovaries (panels A and C, *arrows*, respectively) and absent in adjacent sections incubated with preadsorbed primary antibody (panels B and D, 40× and 100× magnification, respectively). ERKO ovaries at both magnifications demonstrate prominent nuclear staining comparable with that of WT ovaries (panels E and F, *arrows*). Staining for ERα protein was evident in thecal and interstitial cells (panel G, *arrows*), but absent in the granulosa cells of WT ovaries and absent in sections processed without primary antibody (panel H).

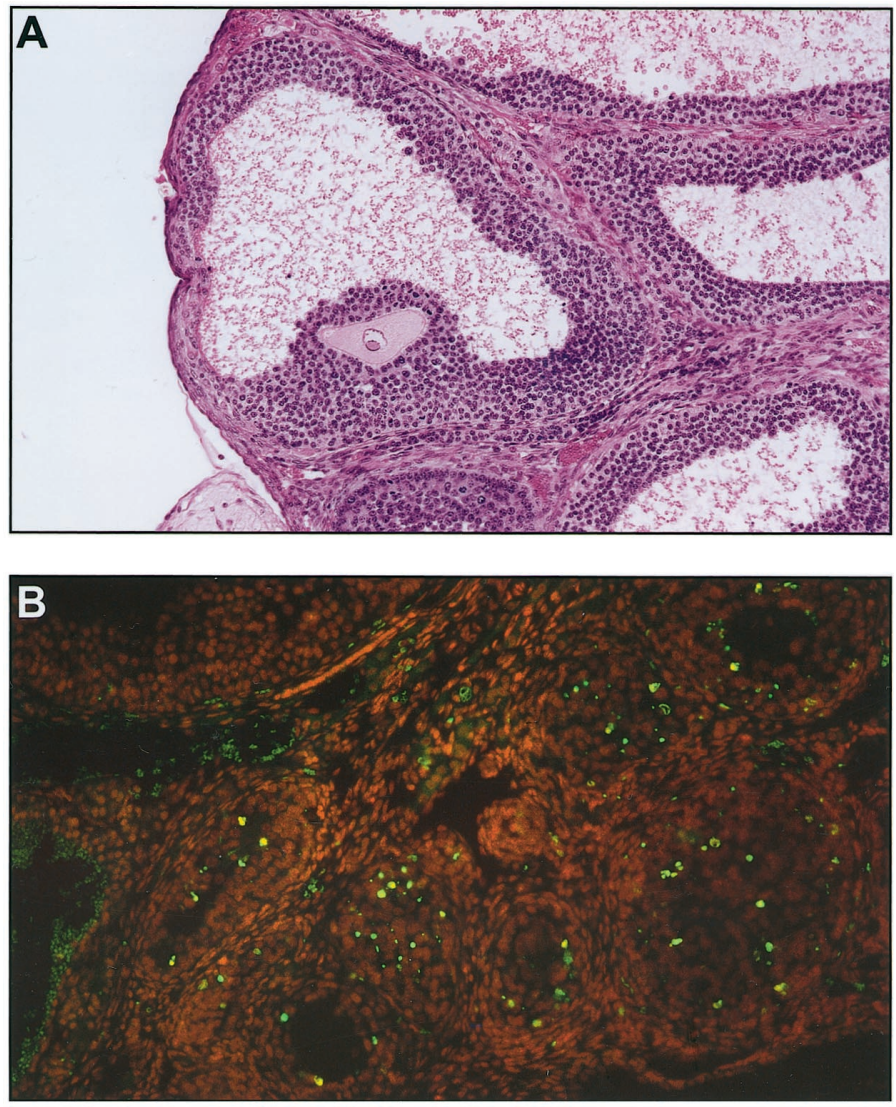

FIG. 7. A, Granulosa cell apoptosis in antral follicles of ERKO ovaries. Representative section of an ERKO ovary showing an atretic mature antral follicle. Granulosa cells with pycnotic, dark-staining nuclei indicative of apoptosis are evident throughout the follicle. Many granulosa cells have sloughed into the follicular fluid and lysed. The oocyte is degenerating. Follicles surviving beyond this stage typically become cystic. B, Representative section of an ERKO ovary demonstrating apoptotic granulosa cells using a TUNEL-based fluorescent label. Apoptotic cells are *yellow-green*.

ERβ mRNA is highly expressed in granulosa cells and it is a likely candidate to explain the earlier studies that indicated estrogen action was necessary, but not sufficient, for LHR induction (8). LH itself is another candidate effector. Although ovulatory levels of LH transiently down regulate LHR, LH has also been shown to maintain granulosa cell LHR binding (41, 42).

PR knockout mice also fail to ovulate (36). Thus, the action of this receptor is important and potentially very relevant to the ovulatory failure in the ERKOs because ER activity is prerequisite for the induction of at least some forms of PR mRNA expression in the uterus (18). PR mRNA was low but comparable in both genotypes. If PR mRNA expression were ERβ-regulated, one would expect levels to be high in the ERKO because circulating estrogen is elevated in these animals. It is more likely that ovarian PR mRNA expression is regulated by cAMP (43, 44). Our results would be consistent with this observation. Although the lack of PR expression in a specific cell type of the ovary associated with ovulation is theoretically possible, these results also indicate that the anovulatory ERKO phenotype cannot be ascribed to an absence of PR mRNA expression.

Failure of the ovulatory mechanism in the ERKO animals is not due to impairment of steroidogenesis *per se*. The increased androgen and estrogen levels are strong evidence that the rate-limiting steps of StAR, P450scc, and the other P450-dependent steps, C_{17} lyase and aromatase, are not significantly impaired by disruption of the ERα gene (26).

Ovarian ERβ expression was detected at the protein level and it was sharply compartmentalized to the granulosa cells. Granulosa cells of the preantral follicles thus express ERβ as well as FSHR well before expression of LHR binding and mRNA expression (8). ERα gene disruption caused a significant increase in FSHR mRNA levels. This leads to the hypothesis that this receptor may be regulated in part by a combination of ERα and ERβ action or by an ERα/ERβ heterodimer.

The summary findings indicate that the major cause of the adult ERKO phenotype is the disruption in negative feedback at neuroendocrine centers (9), resulting in high circu-

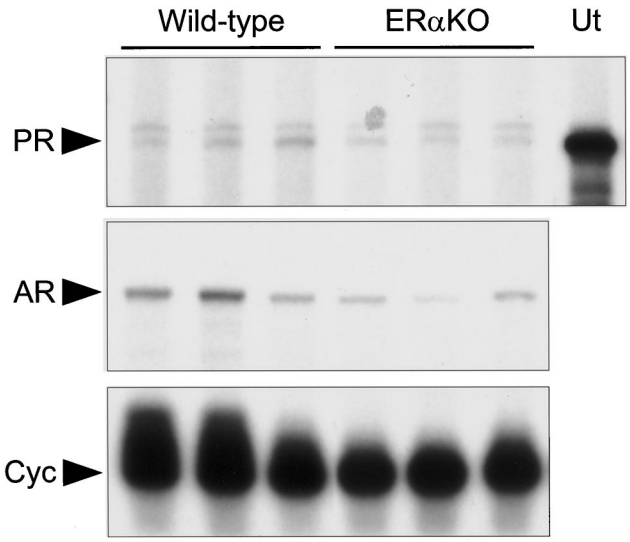

FIG. 8. RNase Protection assay for mRNA encoding the PR and the AR in individual WT and ERKO ovaries. In separate assays, 2.5 μg total ovarian RNA from individual WT and ERKO females was assayed by an RNase protection assay for either PR or AR mRNA as described in the *Materials and Methods*. A riboprobe for cyclophilin mRNA (Cyc) was included in each assay for normalization purposes. For the PR, a sample of WT mouse uterus (Ut) was included to indicate the correct band representing PR mRNA. The PR band (*arrow*) yielded the predicted base pair size products following restriction digest. These panels do not represent equal film exposure for the separate assays.

lating LH interacting with functional ovarian LHR. These processes presumably involve both hypothalamic-pituitary and intraovarian mechanisms dependent upon ERα. Also, ERβ may be preserving roles of estrogen action previously associated with some, but not all of the actions of ERα within the ovary, and ERβ may be uniquely regulating several additional biochemical endpoints that remain to be identified. The ERKO model should therefore be invaluable in helping to dissect the respective roles of these two ERs in ovarian function.

References

1. **Clark JH, Mani SK** 1994 Actions of ovarian steroid hormones. In: Knobil E, Neill JD (eds) The Physiology of Reproduction, ed. 2, Raven Press, Ltd., New York, pp 1011- 1059
2. **Richards JS, Midgley AR Jr** 1976 Protein hormone action: a key to understanding ovarian follicular and luteal cell development. Biol Reprod 14:82–94
3. **Hurst BS, Zilberstein M, Chou JY, Litman B, Stephens J, Leslie KK** 1995 Estrogen receptors are present in human granulosa cells. J Clin Endocrinol Metab 80:229–232
4. **Goldenberg RL, Vaitukaitis JL, Ross GT** 1972 Estrogen and follicle stimulating hormone interactions on follicle growth in rats. Endocrinology 90:1492–1498
5. **Mulheron GW, Schomberg DW** 1992 Effects of diethylstilbestrol on rat granulosa cell and thecal/interstitial cell transforming growth factor-β2 mRNA expression *in vivo*: analysis by reverse transcription-polymerase chain reaction. Biol Reprod 46:546–550
6. **Billig H, Furuta I, Hsueh AJW** 1993 Estrogens inhibit and androgens enhance ovarian granulosa cell apoptosis. Endocrinology 133:2204–2212
7. **Wiesen JF, Midgley AR Jr** 1993 Changes in expression of connexin 43 gap junction messenger ribonucleic acid and protein during ovarian follicular growth. Endocrinology 133:741–746
8. **Richards JS** 1980 Maturation of ovarian follicles: actions and interactions of pituitary and ovarian hormones on follicular cell differentiation. Physiol Rev 60:51–89
9. **Scully KM, Gleiberman AS, Lindzey J, Lubahn DB, Korach KS, Rosenfeld MG** 1997 Role of estrogen receptor α in the anterior pituitary gland. Mol Endocrinol 11:674–681
10. **Lindzey J, Couse JF, Stoker T, Wetsel WC, Copoper R, Korach KS,** Steroid regulation of gonadotrope function in wild-type (WT) and estrogen receptor-α (ERKO) mice. Program of the 80th Annual Meeting of The Endocrine Society, New Orleans, LA, 1998 (Abstract OR46-2), p 112
11. **Lubahn DB, Moyer JS, Golding TS, Couse JF, Korach KS, Smithies O** 1993 Alteration of reproductive function but not prenatal sexual development after insertional disruption of the mouse estrogen receptor gene. Proc Natl Acad Sci USA 90:11162–11166
12. **Dukes M, Chester R, Yarwood L, Wakeling AE** 1994 Effects of a non- steroidal pure antioestrogen, ZM 189,154, on oestrogen target organs of the rat including bones. J Endocrinol 141:335–341
13. **Luo S, Martel C, Souria A, Cauthier S, Morand Y, Belanger A, Labrie C, Labrie F** 1997 Comparative effects of 28-day treatment with the new antiestrogen EM-800 and tamoxifen on estrogen-sensitive parameters in intact mice. Int J Cancer 73:381–391
14. **Sourla A, Luo S, Labire C, Belanger A, Labrie F** 1997 Morphological changes induced by 6-month treatment of intact and ovariectomized mice with tamoxifen and the pure antiestrogen EM-800. Endocrinology 138:5605–5617
15. **Kuiper GGJM, Enmark E, Pelto-Huikko M, Nilsson S, Gustafsson J-A** 1996 Cloning of a novel estrogen receptor expressed in rat prostate and ovary. Proc Natl Acad Sci USA 93:5925–5930
16. **Byers M, Kuiper GGJM, Gustafsson J-A, Park-Sarge O-K** 1997 Estrogen receptor-β mRNA expression in rat ovary: down-regulation by gonadotropins. Mol Endocrinol 11:172–181
17. **Couse JF, Lindzey J, Grandien K, Gustafsson J-A, Korach KS** 1997 Tissue distribution and quantitative analysis of estrogen receptor-α (ERα) and estrogen receptor-β (ERβ) messenger ribonucleic acid in the wild-type and ERα-knockout mouse. Endocrinology 138:4613–4621
18. **Couse JF, Curtis SW, Washburn TF, Lindzey J, Golding TS, Lubahn DB, Smithies O, Korach KS** 1995 Analysis of transcription and estrogen insensitivity in the female mouse after targeted disruption of the estrogen receptor gene. Mol Endocrinol 9:1441–1454
19. **Mor G, Amir-Zaltsman Y, Barnard G, Kohen F** 1992 Characterization of an antiidiotypic antibody mimicking the actions of estradiol and its interaction with estrogen receptors. Endocrinology 130:3633–3640
20. **Sar M** 1985 Application of avidin and biotin technique for the localization of estrogen receptor in target tissues using monoclonal antibodies. In: Bullock GR, Petrusz P (eds) Techniques in Immunocytochemistry, vol 3, Academic Press, New York, pp 43–54
21. **Park OK, Mayo KE** 1991 Transient expression of progesterone receptor messenger RNA in ovarian granulosa cells after the preovulatory luteinizing hormone surge. Mol Endocrinol 5:967–978
22. **Couse JF, Korach KS** 1998 Exploring the role of sex steroids through studies of receptor deficient mice. J Mol Med 76:497–511
23. **LaPolt PS, Tilly JL, Aihara Y, Nishimori K, Hsueh AJ** 1992 Gonadotropin-induced up-and down-regulation of ovarian follicle-stimulating hormone (FSH) receptor gene expression in immature rats: effects of pregnant mare's serum gonadotropin, human chorionic gonadotropin, and recombinant FSH. Endocrinology 130:1289–1295
24. **Heckert LL, Griswold MD** 1991 Expression of Follicle-stimulating Hormone receptor mRNA in rat testes and Sertoli cells. Mol Endocrinol 5:670–677
25. **Segaloff DL, Ascoli M** 1993 The lutropin/choriogonadotropin receptor . . . 4 years later. Endocr Rev 14:324–347
26. **Lindzey J, Korach KS** 1997 Developmental and physiological effects of estrogen receptor gene disruption in mice. Trends Endocrinol Metab 8:137–145
27. **Dong J, Albertini DF, Nishimori K, Kumar TR, Lu N, Matzuk MM** 1996 Growth differentiation factor-9 is required during early ovarian folliculogenesis. Nature 383:531–535
28. **Kumar TR, Wang Y, Lu N, Matzuk MM** 1997 Follicle stimulating hormone is required for ovarian follicle maturation but not male fertility. Nat Genet 15:201–201
29. **Zhou J, Kumar TR, Matzuk MM, Bondy C** 1997 Insulin-like growth factor I regulates gonadotropin responsiveness in the murine ovary. Mol Endocrinol 11:1924–1933
30. **Sicinski P, Donaher JL, Geng Y, Parker SB, Gardner H, Park MY, Robker RL, Richards JS, McGinnis LK, Biggers JD, Eppig JJ, Bronson RT, Elledge SJ, Weinberg RA** 1996 Cyclin D2 is an FSH-responsive gene involved in gonadal cell proliferation and oncogenesis. Nature 384:47–474
31. **Lim H, Paria BC, Das SK, Dinchuk JE, Langenbach R, Trzaskos JM, Dey SK** 1997 Multiple female reproductive failures in cyclooxygenase 2-deficient mice. Cell 91:197–208
32. **Yoshizawa T, Handa Y, Uematsu Y, Takeda S, Sekine K, Yoshihara Y, Kawakami T, Karioka K, Sato H, Uchiyama Y, Masushige S, Fukamizu A, Matsumoto T, Kato S** 1997 Mice lacking the vitamin D receptor exhibit impaired bone formation, uterine hyperplasia and growth retardation after weaning. Nat Genet 16:391–396
33. **Guo Q, Kumar TR, Woodruff T, Hadsell LA, DeMayo FJ, Matzuk MM** 1998 Overexpression of mouse Follistatin causes reproductive defects in transgenic mice. Mol Endocrinol 12:96–106
34. **Fisher CR, Graves KH, Parlow AF, Simpson ER** 1998 Characterization of mice

deficient in aromatase (ArKO) because of targeted disruption of the cyp19 gene. Proc Natl Acad Sci USA 95:6965–6970
35. **Alexander SM, Goodenough DA, Li E, Paul DL** 1997 Female infertility in mice lacking connexin 37. Nature 385:525–529
36. **Lydon JP, DeMayo FJ, Funk CR, Mani SK, Hughes AR, Montgomery Jr CA, Shyamala G, Conneely OM, O'Malley BW** 1995 Mice lacking progesterone receptor exhibit pleiotropic reproductive abnormalities. Genes Dev 9:2266–2278
37. **Shupnik MA** 1998 Gonadal hormone feedback on pituitary gonadotropin genes. Trends Endocrinol Metab 7:272–276
38. **Wilson ME, Price Jr RH, Handa RJ** 1998 Estrogen receptor-β messenger ribonucleic acid expression in the pituitary gland. Endocrinology 139:5151-5156
39. **Risma KA, Clay CM, Nett TM, Wagner T, Yun J, Nilson JH** 1995 Targeted overexpression of luteinizing hormone in transgenic mice leads to infertility, polycystic ovaries, and ovarian tumors. Proc Natl Acad Sci USA 92:1322–1326
40. **Risma KA, Hirshfield AN, Nilson JH** 1997 Elevated LH in prepubertal transgenic mice causes hyperandrogenimia, precocious puberty, and substantial ovarian pathology. Endocrinology 138:3540–3547
41. **LaPolt PS, Oikawa M, Jia XC, Dargan C, Hsueh AJ** 1990 Gonadotropin-induced up- and down-regulation of rat ovarian LH receptor message levels during follicular growth, ovulation and luteinization. Endocrinology 126:3277-3279
42. **Piquette GN, LaPolt PS, Oikawa M, Hsueh AJ** 1991 Regulation of luteinizing hormone receptor messenger ribonucleic acid levels by gonadotropins, growth factors, and gonadotropin-releasing hormone in cultured rat granulosa cells. Endocrinology 128:2449–2456
43. **Park-Sarge O-K, Mayo KE** 1994 Regulation of the progesterone receptor gene by gonadotropins and cyclic adenosine 3′,5′-monophosphate in rat granulosa cells. Endocrinology 134:709–718
44. **Clemens JW, Robker RL, Kraus WL, Katzenellenbogen BS, Richards JS** 1998 Hormone induction of progesterone receptor (PR) messenger ribonucleic acid and activation of PR promoter regions in ovarian granulosa cells: Evidence for a role of cyclic adenosine 3′5′-mono-phosphate but not estradiol. Mol Endocrinol 12:1201–1214